

of Shackleton<sup>4</sup>, are not observed within the crater floors visible to the Arecibo system. Any ice in these regions must be in the form of disseminated grains or thin (centimetres or less) interbedded layers, which could satisfy the Lunar Prospector results without strong radar backscatter enhancement.

This type of ice deposit, if present, would be considerably different from the thick, coherent layers observed in shadowed craters on Mercury<sup>7,8</sup>. Such 'sparse' filling of the lunar cold-traps relative to Mercury could arise as a result of a lower average delivery rate of comets to the Moon, fortuitous recent comet impacts on Mercury, or a more rapid loss of ice on the lunar surface.

**Bruce A. Campbell\***, **Donald B. Campbell†**, **John F. Chandler‡**, **Alice A. Hine§**, **Michael C. Nolan§**, **Phillip J. Perillat§**

\*Center for Earth and Planetary Studies, Smithsonian Institution, Box 37012, Washington DC 20013-7012, USA  
e-mail: campbellb@nasn.si.edu

†Cornell University, Space Sciences Building, Ithaca, New York 14853, USA

‡Smithsonian Astrophysical Observatory, Cambridge, Massachusetts 02138, USA

§Arecibo Observatory, HC3 Box 53995, Arecibo 00612, Puerto Rico

- Margot, J. L., Campbell, D. B., Jurgens, R. F. & Slade, M. A. *Science* **284**, 1658–1660 (1999).
- Bussey, D. B. J., Spudis, P. D. & Robinson, M. S. *Geophys. Res. Lett.* **26**, 1187–1190 (1999).
- Nozette, S. *et al. Science* **274**, 1495–1497 (1996).
- Nozette, S. *et al. J. Geophys. Res.* **106**, 23253–23266 (2001).
- Feldman, W. C. *et al. J. Geophys. Res.* **106**, 23232–23252 (2001).
- Black, G. J., Campbell, D. B. & Nicholson, P. D. *Icarus* **151**, 167–180 (2001).
- Harmon, J. K. *et al. Nature* **369**, 213–215 (1994).
- Black, G. J., Campbell, D. B. & Harmon, J. K. *Lunar Planet Sci. Conf. XXXIII* abstr. 1946 (2002).
- Stacy, N. J. S., Campbell, D. B. & Ford, P. G. *Science* **276**, 1527–1530 (1997).

Competing financial interests: declared none.

Astrophysics

## Refreshed shocks from a $\gamma$ -ray burst

In addition to its remarkable supernova signature<sup>1,2</sup>, the  $\gamma$ -ray burst of 29 March 2003 (GRB030329) had two interesting peculiarities: an unusually low-energy output in  $\gamma$ -rays and a large bump in its afterglow light curve after 1–2 days (followed by several less significant rebrightening episodes). We suggest that refreshed shocks — slow shells ejected from the source that catch up with the afterglow shock a relatively long time after the initial burst — produced the observed fluctuations in the early afterglow light curve and explain the low-energy output at early times.

The  $\gamma$ -ray emission in GRBs is thought to arise from internal shocks within a relativistic outflow from a compact source, which occur as different 'shells' within the outflow collide with each other (Fig. 1). At a greater distance,  $R$ , from the source, the ejecta decelerates as it

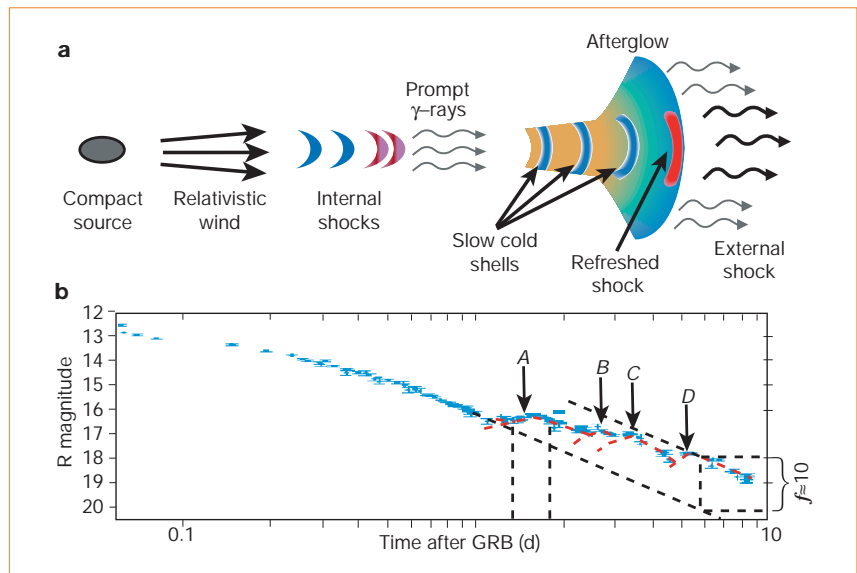


**Figure 1** Refreshed shocks in  $\gamma$ -ray bursts. **a**, Illustration of a  $\gamma$ -ray burst: a compact source ejects a variable relativistic wind. Internal shocks within the outflow produce the  $\gamma$ -rays. At greater distances, the ejecta drives a strong shock into the surrounding medium, producing the afterglow. Slow shells ejected from the source catch up with the afterglow shock at late times, producing refreshed shocks; they thereby energize the afterglow and cause bumps in its light curve. **b**, Light curve of the GRB030329 burst (see <http://lanl.arxiv.org/abs/astro-ph/0304563> for refs) shows a large bump (A, red line) at  $t \approx 1.3$ – $1.7$  d, followed by three less significant bumps (B–D, dashed red lines, at  $t \approx 2.4$ – $2.8$  d,  $t \approx 3.1$ – $3.5$  d and  $t \approx 4.9$ – $5.7$  d, respectively).

drives a strong shock into the surrounding medium, producing the subsequent afterglow.

The achromatic increase in steepness of the optical light curve of GRB030329, from  $t^{-\alpha}$ , where  $t$  is the time measured from the burst, with  $\alpha = \alpha_1 = 0.873 \pm 0.025$  at  $t < t_j \approx 40.481 \pm 0.333$  days to  $\alpha = \alpha_2 = 1.97 \pm 0.12$  at  $t > t_j$  (ref. 3), resembled jet breaks seen in other GRBs. The inferred opening angle implies a prompt  $\gamma$ -ray energy output,  $E_\gamma$ , and X-ray luminosity at 10 h,  $L_x$ , that are factors of roughly 20 and 30, respectively, below the average values around which most GRBs are narrowly clustered<sup>3</sup>.

A well-monitored rebrightening with an amplitude  $f \approx 2$  is evident at  $t \approx 1.3$ – $1.7$  days (Fig. 1), with a duration  $\Delta t \approx t_j < t$ . After the bump, the slope returns to  $\alpha \approx \alpha_1$ . Three additional, less significant bumps with similar features follow.

Angular smoothing generally suggests that light-curve variations should have  $\Delta t \geq t$ . However, here  $\Delta t < t$ . External density variations and patchy shells, which have been proposed to explain other variable afterglows, do not work here. The former requires an unrealistic external density; the latter fails because in GRB030329 the bumps occur after  $t_j$ , when the entire jet is visible.

Refreshed shocks (Fig. 1) arise when slow shells catch up with the afterglow shock at late times<sup>4–6</sup>. Each collision causes a rebrightening in the afterglow light curve. After the rebrightening, the afterglow resumes its original decay slope. The stepwise shape of the light curve for GRB030329, where the same slope,  $\alpha_2$ , is regained after each bump, is a clear signature of refreshed shocks.

The collisions also inject energy into the afterglow shock. An energy increase of a factor  $f$  increases the flux normalization by a factor  $f = f^{(3+p)/4}$  for  $v_m < v < v_c$  and  $f = f^{(2+p)/4}$  for  $v > v_m, v_c$ , where  $p$  is the electron power-law index and  $v_c(v_m)$  is the cooling (typical) frequency. For GRB030329,  $p \approx 2$  and  $v_c(t_j)$  is around the optical<sup>3</sup>, so  $f$  is roughly linear in  $f$ . The observed  $f \approx 10$  (Fig. 1) implies  $f \approx 10$ , which brings the total energy close to the average value for all GRBs.

The original refreshed-shocks scenario<sup>5</sup> predicts  $\Delta t \approx t$ . However, this assumes that refreshed shocks occur before  $t_j$ , whereas in GRB030329 they took place after  $t_j$ . As the later shells move in the wake of the forward shock, they remain cold and do not expand sideways. If all the shells have the same initial half-opening angle,  $\theta_0$ , the duration of the rebrightening events will be  $\Delta t \approx R\theta_0^2/2c = t_j(R/R_j) = t_j(t/t_j)^b$ , where  $b = 1/4$  ( $b \approx 0$ ) if the lateral spreading of the jet is negligible (at the local sound speed). This allows  $\Delta t < t \approx R/2\gamma^2 c$ . Also, the width of the rear shell must be smaller than  $c\Delta t$ .

Numerical simulations suggest rather modest lateral spreading<sup>7</sup>, implying  $b \approx 1/4$ . This is consistent with  $\Delta t \approx t_j$  for the first bump (and with  $\Delta t \approx t_j, 2t_j, 2t_j$  for the later bumps). The energy increase after each refreshed shock causes a more rapid consequent increase in  $R$ ; the overall effect, however, is a factor  $\leq 2$ . The timing of the first bump suggests a Lorentz factor of about 6 for the slower shell.

Refreshed shocks can explain both the variability and the anomalously low values inferred for  $E_\gamma$  and  $L_x$ . A direct prediction of this interpretation is that there will be significant radio flares that correspond to the

observed optical bumps. These should arise from emission by the reverse shocks that form in the refreshed shocks.

**Jonathan Granot\***, **Ehud Nakar†**, **Tsvi Piran†**

\**Institute for Advanced Study, Princeton, New Jersey 08540, USA*

†*Racah Institute for Physics, The Hebrew University, Jerusalem 91904, Israel*

e-mail: [udini@phys.huji.ac.il](mailto:udini@phys.huji.ac.il)

1. Stanek, K. Z. *et al. Astrophys. J.* **591**, L17–L20 (2003).
2. Hjorth, J. *et al. Nature* **423**, 847–850 (2003).
3. Price, P. A. *et al. Nature* **423**, 844–847 (2003).
4. Rees, M. J. & Mészáros, P. *Astrophys. J.* **496**, L1–L4 (1998).
5. Kumar, P. & Piran, T. *Astrophys. J.* **532**, 286–293 (2000).
6. Sari, R. & Mészáros, P. *Astrophys. J.* **535**, L33–L37 (2000).
7. Granot, J., Miller, M., Piran, T., Suen, W. M. & Hughes, P. A. in *Gamma-Ray Bursts in the Afterglow Era* (eds Costa, E., Frontera, F. & Hjorth, J.) 312–314 (Springer, Berlin, 2001).

Competing financial interests: declared none.

COMMUNICATIONS ARISING

Astrophysics

## A constraint on canonical quantum gravity?

Gamma rays from the  $\gamma$ -ray burst (GRB) 021206 have been reported to be strongly linearly polarized<sup>1</sup>, with the estimated degree of polarization ( $80 \pm 20\%$ ) being close to the absolute maximum of 100% — affording us the opportunity to constrain models of quantum gravity, which has had  $10^{10}$  years to act on the photons as they travelled towards us. Here I show that if the effects of quantum gravity are linearly proportional to the ratio of the photon energy to the characteristic scale energy of quantum gravity, then the polarization of photons with energies of about 0.1 MeV should be completely random, contrary to what is observed. I conclude that, should the polarization measurement be confirmed, quantum gravity effects act with a power that is greater than linearity, or that loop quantum gravity is not viable. Compared with previous methods and results (see ref. 2, for example), testing of the linear polarization of cosmic  $\gamma$ -ray bursts may substantially extend the observational window on the theory of quantum gravity.

GRBs are characterized by a highly variable flux of high-energy photons that propagate over cosmological distances. It has been suggested<sup>3</sup> that they are the best candles in cosmological space, allowing us either to study or to constrain the effects of quantum gravity. These effects are known<sup>3,4</sup> to be proportional to the ratio  $(E/E_{\text{QG}})^n$  of the photon energy,  $E$ , to the Planck energy,  $E_{\text{QG}} \approx 10^{19}$  GeV, and to the distance,  $D$ , of the photon's propagation. The linear case ( $n=1$ ) is the best studied<sup>3,4</sup>, but the quadratic case ( $n=2$ ) has also recently been considered (see preprint at [http://xxx.lanl.gov/PS\\_cache/gr-qc/pdf/0305/0305057.pdf](http://xxx.lanl.gov/PS_cache/gr-qc/pdf/0305/0305057.pdf)). For  $n=1$ , the effect of the energy-dependent refraction of

photons in quantum space-time should lead to a measurable difference in arrival time (of the order of milliseconds) for photons with different energies<sup>2</sup>.

The linear polarization of  $\gamma$ -rays from GRB 021206 allows us to test another possible effect of quantum space-time, which is predicted for canonical quantum gravity in loop representation. In this case, space-time exhibits the property of birefringence<sup>4</sup>: two photons with opposite states of helicity,  $+1$  and  $-1$ , have different group velocities

$$v_{\pm} = c(1 \pm \chi(E/E_{\text{QG}})^n) \quad (1)$$

The factor  $\chi$  is about 1 for loop representation of quantum gravity<sup>3</sup>. A linearly polarized electromagnetic wave may be represented as the superposition of two monochromatic waves with opposite circular polarizations. When a linearly polarized wave propagates inside the substance with birefringence, the plane of polarization rotates along the path because of the difference in group velocity between the two circular components.

For the linear case  $n=1$ , the phase angle,  $\varphi_1$ , of a plane of linear polarization changes along a distance  $D$  (in light years) as

$$\Delta\varphi_1(E) \approx \chi(D/hc)E^2/E_{\text{QG}} \approx 10^4 \chi (E/0.1 \text{ MeV})^2 D \quad (2)$$

This angle depends on the photon energy as  $E^2$ . Linear polarization measured within a broad energy range should vanish, provided that the difference in accumulated angles is large for photons with different energies. Two photons with energies of around 0.1 MeV and with a difference of energy of about 0.01% will therefore accumulate a difference of  $\delta\varphi \approx \chi$  in polarization phase angle after a year of propagation in space with birefringence (see equation (2)).

For cosmological GRBs, which have a travel distance of  $D \approx 10^{10}$  light years, the planes of linear polarization of photons with different energies should be totally randomized. The bulk linear polarization of photons with energies greater than 0.01 eV over a broad energy range must become zero even if they were all originally 100% polarized in a single plane.

In the quadratic case of quantum space-time birefringence with  $n=2$ , the rotation of a plane of linear polarization is rather small for photons with energy of around 0.1 MeV

$$\Delta\varphi_2(E) \approx \chi(D/hc)E^3/E_{\text{QG}}^2 \approx 10^{-19} \chi (E/0.1 \text{ MeV})^3 D \quad (3)$$

However, the distance  $D \approx 10^{10}$  light years is so large that even the quadratic case of birefringence could be tested by polarization measurements of photons with energies greater than 100 MeV. The detection<sup>5</sup> of a high-energy component of GRB941017 (energies up to 200 MeV), which dominates the total fluence of the event, suggests that

quadratic space-time birefringence could be tested experimentally in the future by polarimetry of such GRBs.

I therefore conclude that either the birefringence of quantum space-time with  $n=1$  should be below the level of  $\chi > 10^{-14}$ , or it should be quadratic ( $n=2$ ), assuming that the strong linear polarization of GRBs is confirmed by a second measurement.

**Igor G. Mitrofanov**

*Space Research Institute, Profsojuznaya str. 84/32, 117997 Moscow, Russia*

e-mail: [imitrofa@space.ru](mailto:imitrofa@space.ru)

1. Colburn, W. & Boggs, S. E. *Nature* **423**, 415–417 (2003).
2. Jacobson, T., Liberati, D. & Mattingly, D. *Nature* **424**, 1019–1021 (2003).
3. Amelino-Gamella, G., Ellis, J., Mavromatos, N. E., Nanopoulos, D. V. & Sarkar, S. *Nature* **393**, 763–765 (1998).
4. Gambini, R. & Pullin, J. *Phys. Rev. D* **59**, 124021 (1999).
5. Gonzalez, M. M. *et al. Nature* **424**, 749–751 (2003).

COMMUNICATIONS ARISING

Condensed-matter physics

## Spurious magnetism in high- $T_c$ superconductor

One challenge in condensed-matter physics is to unravel the interplay between magnetism and superconductivity in copper oxides with a high critical temperature ( $T_c$ ). Kang *et al.*<sup>1</sup> claim to have revealed a quantum phase transition from the superconducting to an antiferromagnetic state in the electron-doped material  $\text{Nd}_{2-x}\text{Ce}_x\text{CuO}_4$  (NCCO) based on the observation of magnetic-field-induced neutron-scattering intensity at  $(1/2, 1/2, 0)$ ,  $(1/2, 0, 0)$  and related reflections. Here we argue that the observed magnetic intensity is due to a secondary phase of  $(\text{Nd,Ce})_2\text{O}_3$ . We therefore contend that the effect is spurious and not intrinsic to superconducting NCCO.

To achieve superconductivity in NCCO, a rather severe oxygen-reduction procedure has to be applied<sup>2</sup>. We have discovered that the reduction process decomposes a small (0.01–0.10%) volume fraction of NCCO. The resultant  $(\text{Nd,Ce})_2\text{O}_3$  secondary phase has the complex cubic bixbyite structure, common among rare-earth (RE) sesquioxides<sup>3</sup>, with a lattice constant,  $a_c$ , that is about  $2\sqrt{2}$  times the planar lattice constant of tetragonal NCCO.  $(\text{Nd,Ce})_2\text{O}_3$  is epitaxial with the host lattice, with long-range order parallel to the  $\text{CuO}_2$  planes of NCCO, but extending only about  $5a_c$  perpendicular to the planes. Because of the relationship between the two lattice constants, certain structural reflections from the impurity phase appear at seemingly commensurate NCCO positions — that is, the cubic  $(2, 0, 0)_c$  reflection can also be indexed as  $(1/2, 1/2, 0)$ . However, there is roughly a 10% mismatch between  $a_c$  and the  $c$ -lattice constant of NCCO, and therefore  $(0, 0, 2)_c$  can also be indexed as  $(0, 0, 2.2)$ .